Noise generated by a leading edge in anisotropic turbulence

T. F. Geyer[1], E. Sarradj and M. Hobracht
Chair of Technical Acoustics
Brandenburg University of Technology Cottbus - Senftenberg, Germany

ABSTRACT

The noise generated by the interaction of a turbulent inflow with the leading edge of a flat plate or an airfoil is a dominant sound source, for example in rotor-stator configurations of fans and air condition units. Aeroacoustic research of this noise source often includes performing wind tunnel experiments, where the required incident turbulence is generated by passive grids or meshes. In certain cases, for example in close proximity to the grid, the generated turbulence may be anisotropic and inhomogeneous.

In the present experimental study, constant temperature measurements were performed both in isotropic, homogeneous turbulence as well as in anisotropic, inhomogeneous turbulence. The results were used as an input for a common turbulence interaction noise prediction model and compared with acoustic measurements both on a flat plate and a NACA 0012 airfoil. When turbulence measurements are performed at several measurement positions to account for the inhomogeneity, the model delivers usable results for inhomogeneous and anisotropic turbulence as well. For measurements on airfoils of finite thickness, common thickness corrections should be used. Finally, a larger set of acoustic measurements were performed. The results of these measurements were scaled based on the dependencies on the parameters of the turbulence as used in the prediction model.

Keywords: Turbulence interaction noise, Leading edge, Turbulence, Wind tunnel

1. INTRODUCTION

Turbulence interaction noise is a main aeroacoustic noise source mechanism. It often dominates the noise generation, as for example in rotor-stator configurations of fans and air condition units. Besides numerical models, there exist a number of analytical models for the prediction of this type of noise. Most of these models are based on the assumption of an ideally homogeneous and isotropic turbulence. In a practical situation, however, this assumption may not be justified. For example, when measurements are performed in a wind tunnel where grids, perforated plates or meshes are used to generate a turbulent flow, the resulting turbulence may be inhomogeneous and anisotropic. This is especially true in close proximity to the grids. However, when very high turbulence intensities are desired it may be necessary to perform measurements closer to the grid since the intensity strongly decays with increasing distance.

One well-known model for the prediction of noise generated at the leading edge of a flat plate due to a turbulent inflow is the model from Amiet [1], which was developed based on measurements by Fink [2] on a flat plate of 0.46 m chord. The part of this so called "flat-plate theory" that is used for the prediction of the high-frequency portion of turbulence interaction noise makes use of turbulence intensity Tu, streamwise integral length scale Λ_x and Mach number $Ma = U_\infty/c$ for the description of the turbulent inflow as well as airfoil semi-span h and the distance of the observer R for the description of the experimental configuration only. The high frequency asymptote of the solution in third octave bands, derived by using the Kármán interpolation formula [3] to model the spectrum of the inflow turbulence, is given by

$$L_p = 10 \cdot \log_{10}\left(\frac{\Lambda_x \cdot h}{R^2} \cdot Ma^5 \cdot Tu^2 \cdot \frac{\hat{K}_x^3}{(1+\hat{K}_x^2)^{7/3}}\right) + 181.3 \text{ dB}. \quad (1)$$

Thereby, $\hat{K}_x$ is a normalized chordwise turbulence wavenumber. Amiet's linearized theory is based on the assumption of homogeneous and isotropic turbulence and is valid for an observer located in the acoustic far

[1]email: thomas.geyer@b-tu.de

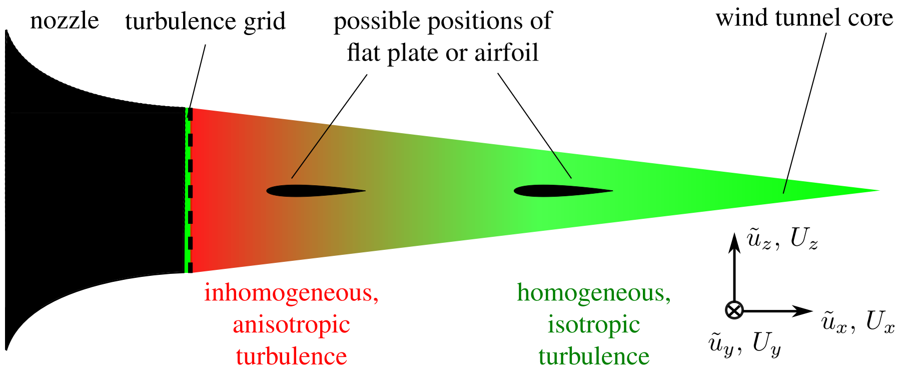

Figure 1: Schematic of the measurement setup in the small aeroacoustic open jet wind tunnel

field. It was found to agree well with the data measured by Fink [2] when the parameter $Ma \cdot K_x \cdot h > 1$, while for lower flow speeds and higher frequencies the model was found to overpredict the leading edge noise due to the fact that the wavelength of the inflow, U_∞ / f, then is in the order of the leading edge radius of the plate or airfoil.

A correction for Amiet's flat-plate theory, that takes into account a finite airfoil thickness, was developed by Gershfeld [4]. The method was validated using experimental results from Paterson and Amiet [5]. Santana et al. [6] provided a low-frequency extension to Amiet's model in order to improve the prediction for compact airfoils. Additionally, the correction developed by Kucukcoskun et al. [7] takes into account a spanwise variation of the incident turbulence.

Although the use of homogeneous and isotropic turbulence in experimental studies is reasonable since it can be statistically described more easily, the turbulence in practical applications may be inhomogeneous and anisotropic. The effect of inhomogeneity and anisotropy on the prediction of Amiet's flat-plate model has not been thoroughly investigated yet. The subject of the present study therefore is a comparison between the prediction using Amiet's flat-plate theory based on Constant Temperature Anemometry (CTA) measurements in both homogeneous, isotropic turbulence and inhomogeneous, anisotropic turbulence with results from acoustic measurements on both a flat plate and a NACA 0012 airfoil model.

2. METHOD

In the experiments described in the present paper, the turbulence was generated by means of grids with square holes mounted to the nozzle of an open jet wind tunnel. To characterize the incoming turbulence generated by one of these grids, preliminary experiments were performed at a single flow speed using a four-wire CTA probe that allows for the calculation of all three velocity components. These measurements were conducted in planes normal to the direction of the flow at two distances from the turbulence grid: (1) in inhomogeneous, anisotropic turbulence, where the turbulence intensity is in the order of 15 %, and (2) in homogeneous, isotropic turbulence with a lower intensity of approximately 4 % (see schematic shown in Fig. 1). The resulting data were then used to calculate turbulence interaction noise using Amiet's flat-plate model. For means of comparison, acoustic measurements were performed on both a flat plate and a NACA 0012 airfoil using microphone array technology and a deconvolution beamforming algorithm.

After these preliminary tests, a larger set of experiments was performed at ten flow speeds using two different turbulence grids. This again included constant temperature anemometry measurements and acoustic measurements using both a flat-plate model and a NACA 0012 airfoil.

2.1 Wind Tunnel

All measurements took place in the small aeroacoustic wind tunnel at Brandenburg University of Technology [8], which is an open jet wind tunnel with a very low background noise as well as a very low turbulence intensity. The experiments were performed using a circular nozzle with an exit diameter of 0.2 m. With this nozzle, and without any turbulence generators, the overall sound pressure level of the background noise for flow speeds up to 50 m/s is below 60 dB(A) and the turbulence intensity directly in front of the nozzle is in

Table 1: Overview of turbulence grids used in the experiments

Grid no.	description	mesh width [mm]	bar width [mm]	porosity [%]
1	PPS 12/2	12	2	0.69
2	PPS 14/4	14	4	0.51

the order of 0.1 %.

In order to examine turbulence interaction noise, different turbulence grids may be mounted to the nozzle exit. In the preliminary tests of the present study, a perforated plate with rectangular holes with a mesh width of 12 mm, a bar width of 2 mm and a thickness of 1 mm was used (corresponding to the first grid in Tab. 1, denoted as PPS 12/2). The resulting grid porosity, defined as the ratio of open area to total area of the grid, is approximately 0.69.

2.2 Characterization of the inflow turbulence

Passive grids, such as arrays of round rods or square bars and perforated plates, are one possible means for the generation of turbulence in wind tunnel studies. Thereby, the turbulence is generated by the single bars of the grid that each generate their own turbulent wake. Downstream of the grid, the turbulent structures from each wake start to mix, until at some distance from the grid the turbulence can be characterized as homogeneous. Simultaneously, the turbulence intensity decreases with increasing distance from the grid.

According to the study by Roach [9], grid generated turbulence can be expected to be homogeneous and isotropic after a distance of approximately ten mesh widths downstream of the grid, which in the present case would correspond to a distance of 0.12 m. Additionally, the grid porosity should be greater than 50 %. In the present study, measurements were performed in planes at two different distances from the nozzle. At the first distance of 0.086 m downstream from the grid the turbulence can be expected to be inhomogeneous and anisotropic. At the second distance of 0.2 m downstream from the grid the turbulence can be expected to be fairly homogeneous and isotropic.

The measurements of the inflow turbulence were performed using constant temperature anemometry with a quad-sensor vorticity probe type AVOP-4-100 made by Auspex Scientific. The velocity data were recorded with a sampling frequency of 25.6 kHz and a total of 256,000 samples, corresponding to a measurement duration of 10 s, using a Dantec multichannel constant temperature anemometry system and 24-Bit data acquisition hardware made by National Instruments. A three-dimensional traverse system with a minimum step size of 0.1 mm was used for the positioning of the probe. In post processing, the first two seconds of each dataset were omitted to avoid the influence of potential vibrations after each halt of the traverse system. For means of comparison, additional hot-wire measurements were performed using a conventional straight Dantec 55P11-type single-wire probe.

The four-wire-probe was calibrated using an approach similar to that proposed by Wittmer et al. [10], where the three velocity components (in x-, y- and z-direction) are calculated from the electric signals of the four wires using predefined error-functions. This calibration includes two separate routines, which are assumed to be independent from each other: First, each of the four wires is velocity-calibrated using a fourth order polynomial fit, which was done at 20 logarithmically distributed velocities between 2 m/s and 60 m/s. The second step is the so-called direct angle calibration, which yields a method to calculate the three velocity components u_x, u_y and u_z from the four voltage signals measured by the four wires. This second routine was performed prior to the measurements using a velocity calibrator model 112700 made by TSI.

The measurement planes at both distances to the turbulence grid were arranged normal to the flow and consisted of 25 points in the horizontal direction × 13 points in the vertical direction (325 points in total) with a distance of 1 mm, and hence spanned an area corresponding to two meshes of the turbulence grid. From these data, the required input parameters for Amiet's flat-plate model were determined. In the most simple form of this model as given by Eq. (1), the only parameters needed to describe the incident turbulence are the turbulence intensity, the flow Mach number (and hence the flow speed) and the streamwise integral length scale.

The turbulence intensity is calculated based on the fluctuating velocity components u_x, u_y and u_z and the mean flow velocity. The mean flow velocity in streamwise direction is equal to the flow speed U_∞, while it can be assumed that the mean flow velocity in the lateral and vertical directions is zero, $U_y = U_z = 0$. Hence the turbulence intensity Tu is given by

$$Tu = \frac{1}{U_\infty}\sqrt{\frac{\overline{\tilde{u}_x^2} + \overline{\tilde{u}_y^2} + \overline{\tilde{u}_z^2}}{3}}, \tag{2}$$

where the tilde denotes the rms value and the overline denotes the time mean. For the case of isotropic turbulence, the three fluctuating velocity components are identical and Eq. (2) reduces to

$$Tu = \frac{\sqrt{\overline{\tilde{u}^2}}}{U_\infty}. \tag{3}$$

Different methods are known for the calculation of the streamwise integral length scale of the turbulence. One procedure that is used very often is based on the determination of the normalized autocorrelation $R(\tau)$ of the velocity fluctuations in streamwise direction measured by a single hot-wire probe,

$$R(\tau) = \frac{\overline{\tilde{u}_x(t) \cdot \tilde{u}_x(t-\tau)}}{\overline{\tilde{u}_x^2}}. \tag{4}$$

To minimize computational cost, the calculation of $R(\tau)$ in the time-domain is often replaced by a calculation of the autospectral density in the frequency domain and a subsequent back-transformation into the time-domain using an Inverse Fast Fourier Transformation (IFFT). Based on the assumption of Taylors "frozen turbulence" hypothesis [3], the autocorrelation $R(\tau)$ is then used to determine an integral time scale according to

$$t_x = \int_0^\infty R(\tau) d\tau. \tag{5}$$

This time can be imagined as the time that the turbulent eddy needs to flow past the hot-wire sensor. In many experimental studies, the integration in Eq. (5) is performed from τ = 0 to the first zero-crossing of the autocorrelation function. The resulting time scale t_x is then multiplied with the mean velocity in the streamwise direction, U_x, to obtain the integral length scale of the turbulence,

$$\Lambda_x = U_x \cdot t_x, \tag{6}$$

which is a measure for the size of the turbulent eddies. The main advantage of this method is that only one hot-wire sensor is needed. In [11, 12], the time scale t_x rather than the length scale Λ_x is used to describe the incidence turbulence. This offers the advantage that the mean flow velocity is not needed, which itself is a quantity to be measured and hence a potential source of error.

A second method to calculate Λ_x, as for example used in [12], is by fitting the one-sided power spectrum of the velocity fluctuations u_x to

$$G_{uu}(f) = \frac{4\tilde{u}_x^2 \Lambda_x}{U_x\left(1 + \left(\frac{2\pi f \Lambda_x}{U_x}\right)^2\right)}, \tag{7}$$

which is a formulation for isotropic and homogeneous turbulence given in [3]. Λ_x can then be obtained from the energy spectrum at f = 0. In the work of Kurian and Fransson [13] it was shown that both methods to calculate Λ_x yield essentially similar results.

There are other calculation routines that require the spatial cross-correlation of the signals from two sensors (cross-correlation method) instead of the autocorrelation of the signal from one hot-wire sensor. This method is often used to determine the lateral integral length scale of the turbulence (the component perpendicular to the mean flow), since it does not require a mean velocity (which is approximately zero in the direction perpendicular to the flow). However, the disadvantage of using this procedure to determine the streamwise integral length scale of the turbulence, besides the general need for a second sensor, is that the presence of the upstream probe affects the properties of the flow field incident to the second one.

To quantify the anisotropy of a turbulent flow, it is reasonable to generate a so-called *anisotropy invariant map* [14]. In such a map, the different states of turbulence can be obtained easily since certain limiting

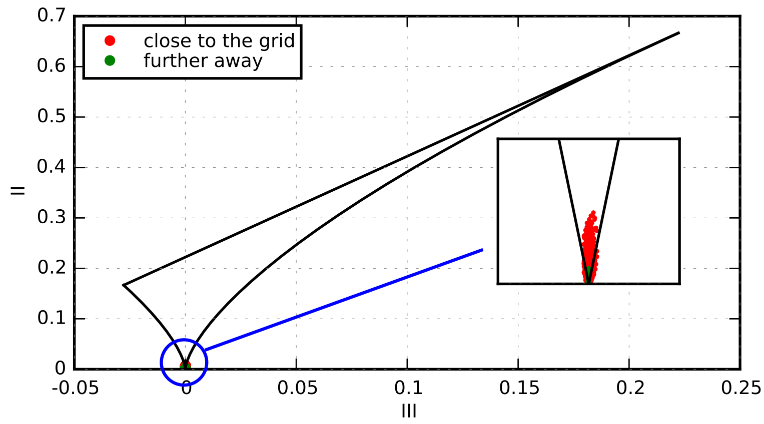

Figure 2: Anisotropy invariant map [14] obtained for the PPS 12/2 turbulence grid at 325 measurement locations at a flow speed of 40 m/s (close to the grid: 0.086 m distance, further away: 0.2 m distance)

states (like completely isotropic turbulence, axisymmetric turbulence or one-component turbulence) define the boundaries of the map. To generate the map, the tensor

$$a_{ij} = \frac{\overline{\tilde{u}_i \tilde{u}_j}}{\overline{\tilde{u}_x^2} + \overline{\tilde{u}_y^2} + \overline{\tilde{u}_z^2}} - \frac{1}{3}\delta_{ij}, \tag{8}$$

and its scalar invariants

$$\begin{aligned} II &= a_{ij}a_{ji}, \\ III &= a_{ij}a_{jk}a_{ki} \end{aligned} \tag{9}$$

have to be calculated and the two invariants can then be plotted in a map [14]. The parameter δ_{ij} in Eq. (8) is the Kronecker delta

$$\delta_{ij} = \begin{cases} 0 & \text{if } i \neq j \\ 1 & \text{if } i = j. \end{cases} \tag{10}$$

Fig. 2 shows the anisotropy invariant map obtained from the measurements with the quad-sensor vorticity probe at a flow speed U_x of approximately 40 m/s at the two distances from the PPS 12/2 turbulence grid. For an ideally isotropic state of the turbulence, the values for the invariants would be located at the origin of the map for each of the 325 single measurements. This is obviously true for the measurements taken further away from the grid at a distance of 0.2 m (which is more than ten mesh widths downstream). The measurements close to the grid (at a distance of 0.086 m, and hence less than ten mesh widths downstream) reveal that the turbulence is not ideally isotropic. However, it can be concluded that even at this shorter distance to the grid the anisotropy of the turbulence is rather weak.

Besides the anisotropy, another property that is of interest for aeroacoustic studies is the homogeneity of the turbulence. Especially at a short distance from the turbulence grid, the existence of regions with particularly low turbulence intensity or particularly high turbulence intensity is possible. This depends on whether the exact measurement location is behind a hole in the grid or behind a grid bar. As an example, Fig. 3 shows the rms value of the three velocity components u_x, u_y and u_z measured at the two distances from the grid. At a distance of only 0.086 m (Fig. 3(a)), distinct regions of high and low velocity are clearly visible, which match the meshes of the turbulence grid. Thus, the turbulence can be described as fairly inhomogeneous. At the greater distance of 0.2 m (Fig. 3(b)), no such regions are visible, characterizing the turbulence as virtually inhomogeneous.

One possibility to take a certain inhomogeneity of the inflow turbulence into account is to average the turbulence characteristics measured at a larger number of locations. In the present case, 325 single measurements were performed at each distance from the grid. This, of course, is too costly in measurement situations where measurements have to be performed either at several distances from the grid or at more than one flow speed. For the present case of inhomogeneity as observed at a distance of 0.086 m from the grid (Fig. 3(a)), an estimate of the influence of the number of measurements n on the resulting averaged values of the flow speed, the turbulence intensity and the integral time scale is given in Fig. 4. The data were obtained by first

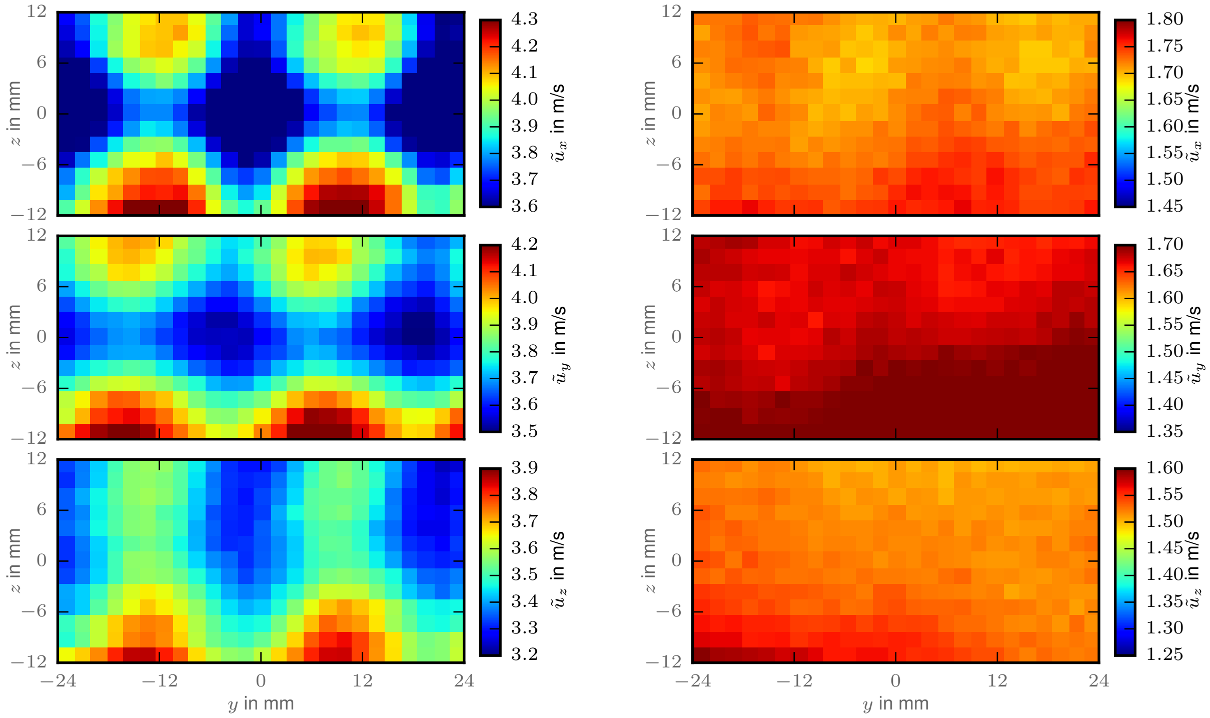

(a) Close to the grid at a distance of 0.086 m

(b) Further away from the grid at a distance of 0.2 m

Figure 3: Components of the turbulent velocity fluctuations at the two distances from the grid

calculating U_∞, Tu (using using Eq. (2)) and t_x (using Eq. (7)) for each of the 325 measurement locations and then averaging the results from n ($n = 1 \ldots 325$) randomly distributed locations. This was repeated ten times to obtain the minima (lower curve) and maxima (upper curve) shown in Fig. 4. It is visible that a very good approximation can already be obtained with only a very small number of measurements. For example, for $n \geq 15$ the average obtained for U_x, Tu and t_x differs less than 2 % from the average obtained from all 325 measurements.

In [11], CTA measurements with a single-wire probe were performed in grid generated turbulence, but at a slightly lager distance from the grid. There it was estimated that measurements at only one position would be necessary to obtain results for $\sqrt{\tilde{\tilde{u}}}$ that lead to differences in sound pressure level according to Eq. (1) of less than 1 dB. Hence, the present investigation further confirms that it is possible to obtain a consistent estimation with only a small number of measurements. In the end, it also has to be considered that, for studies of turbulence interaction noise, the most important parameter characterizing the inflow is the flow speed U_∞, since it appears in Eq. (1) with an exponent of 5.

2.3 Preliminary acoustic measurements

To examine the usability of the predictions of the flat-plate model based on the measured turbulence characteristics, acoustic measurements were performed in the same wind tunnel on both a flat plate and a NACA 0012 airfoil at a flow speed of 40 m/s. The flat plate had a thickness of 0.5 mm, a span width of 0.1 m and a chord length of 0.2 m. The airfoil had the same span, but a chord length of only 0.12 m. The plate (and subsequently the airfoil) were positioned in front of the nozzle. They were fixed to a wooden frame using thin steel wires attached to the edges, which can be seen in Fig. 5. Thus, the models were positioned completely inside the core jet and no noise was generated by the interaction of the wind tunnel shear layer with any part of the models. During acoustic measurements, the test section is surrounded by a cabin equipped with absorbing floor and side walls that provide a quasi-anechoic environment for frequencies approximately above 125 Hz.

In several studies on turbulence interaction noise, such as [2, 5, 15, 16], acoustic measurements were performed using single microphones. In order to eliminate the influence of background noise, such as noise from the fan driving the wind tunnel or from the turbulence generators, it is possible to subtract the back-

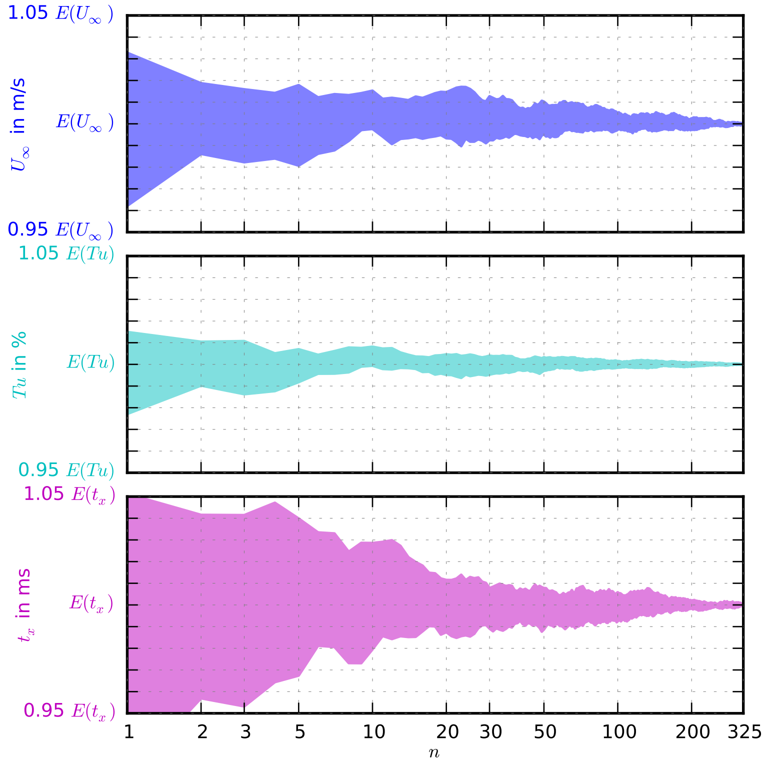

Figure 4: Influence of the number of measurements n on the averages of the flow speed U_∞, the turbulence intensity Tu and the integral time scale t_x (data obtained from n randomly distributed CTA measurements at a distance of 0.086 m from the grid; $E()$ denotes the expected value based on all 325 data points)

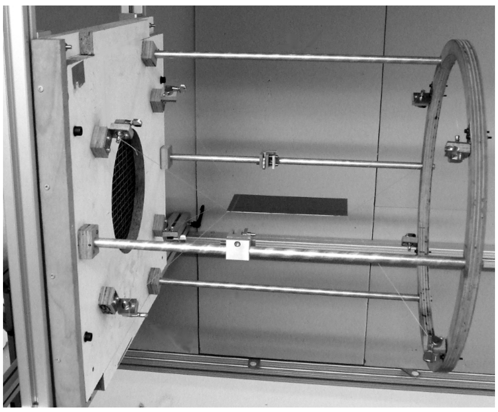

(a) Measurements on flat plate

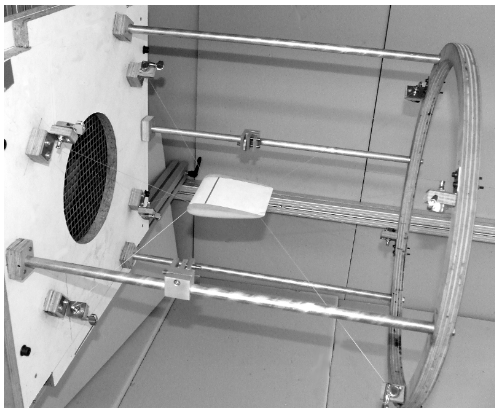

(b) Measurements on NACA 0012 airfoil

Figure 5: Photographs of the acoustic measurement setup used for comparison with the predictions

ground noise levels from the measured data. However, with this method it is not possible to determine the exact location of the noise sources on the airfoil. For example, besides the noise generated by the inflow turbulence interacting with the leading edge of the airfoil, the noise measured by the microphone may also contain noise generated by the interaction of the turbulent boundary layer with the trailing edge. Another, more advanced method is the use of microphone array technology, which enables the separation of noise sources. This is especially important when a high turbulence intensity is desired and hence measurements are performed relatively close to the grid. In the present study, the acoustic measurements were performed using a planar microphone array positioned out of flow above the flat plate/airfoil, consisting of 56 1/4th inch microphone capsules flush-mounted in an aluminum plate of 1.5 m × 1.5 m.

The microphone array data were recorded with a measurement duration of 40 s and a sampling frequency of 51.2 kHz. The time-domain data were Fast-Fourier-transformed into the frequency domain, which was

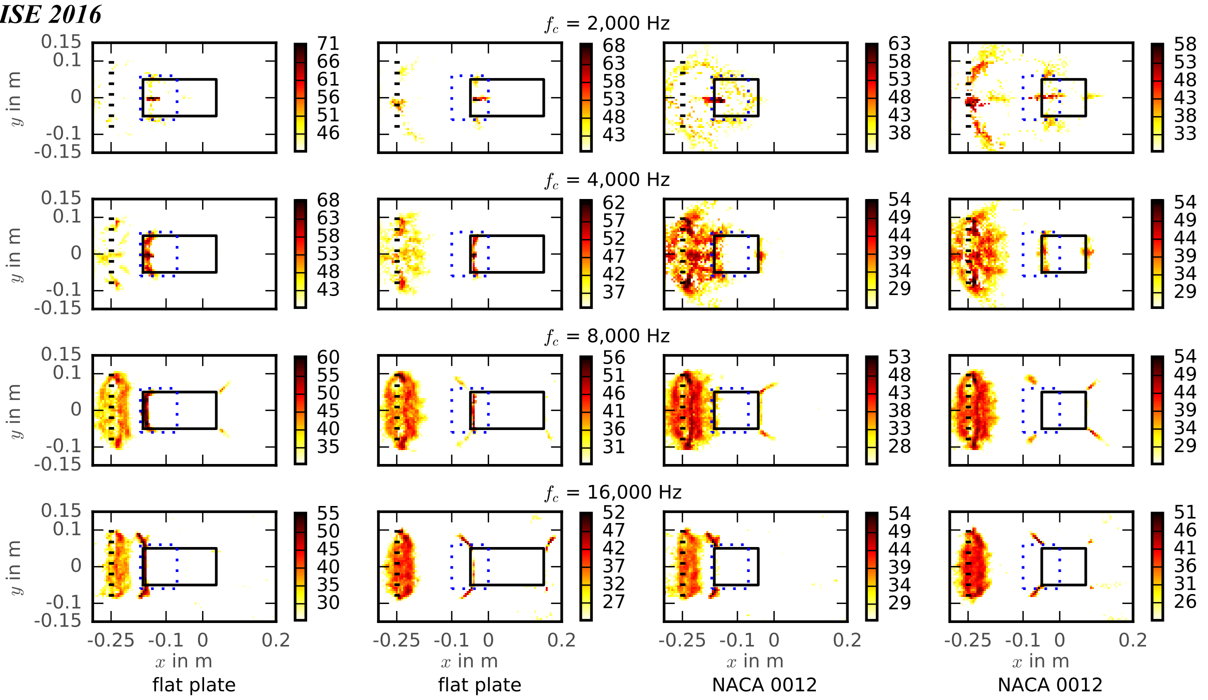

Figure 6: CLEAN-SC octave band sound maps obtained at a flow speed of 40 m/s (first and third column: anisotropic, inhomogeneous turbulence; second and fourth column: isotropic, homogeneous turbulence; black dotted line: turbulence grid, black rectangle: flat plate/airfoil, blue dotted rectangle: integration sector)

done using a Hanning window on 50 % overlapping blocks of 4,096 samples. The resulting spectra were averaged to yield the cross-spectral matrix. For the further processing of the data, different beamforming algorithms were tested. It was finally decided to use the CLEAN-SC algorithm [17] due to its fast performance and overall good results over a wide range of frequencies [18]. The beamforming was applied to a two-dimensional focus plane, where the dimensions of the corresponding focus grid were 0.55 m (chordwise direction) × 0.4 m (spanwise direction) with a resolution of 5 mm, resulting in 8,991 grid points. The main diagonal of the cross-spectral matrix was removed since it contains uncorrelated background noise (for example from the electronic signal processing), but no additional information on the noise sources of interest. The chosen steering vector corresponds to formulation III in [19], which is known to give the correct strength of the noise source, but a slight error in the estimated source location. Additionally, the effects due to the refraction of sound at the shear layers of the open jet was corrected using a fast ray tracing approach [20]. The basic result of the beamforming is a two-dimensional map of noise sources. To obtain quantitative data on the turbulence interaction noise, the contributions from sources within the region of the map that contains the leading edge of the flat plate/airfoil are integrated. Unwanted contributions from other noise sources, such as the wind tunnel nozzle or the trailing edge, were excluded. The results were then converted to third octave band sound pressure levels and 6 dB were subtracted to account for the planar microphone array.

Fig. 6 shows octave band soundmaps obtained for both the flat plate and the airfoil at the two different distances from the turbulence grid. It is visible that a main noise source is located at the leading edge, while additional noise sources are visible at the trailing edge, at the turbulence grid and, in the octave bands with center frequencies of 8 kHz and 16 kHz, at the thin wires that hold the flat plate/airfoil. The noise generated by the turbulence grid becomes very strong at high frequencies. When the flat plate/airfoil is located close to the grid at a distance of only 0.086 m, it is hard to separate the noise generated the leading edge from that generated by the turbulence grid.

During the preliminary acoustic measurements, the effect of a tripping device (a thin strip of tape applied to both suction side and pressure side of the plate/airfoil at approximately 10 % of the chord) was examined. It was found that the tripping had no influence on the source location and the amplitude of the generated turbulence interaction noise, which is in agreement with other studies on that noise source mechanism (for

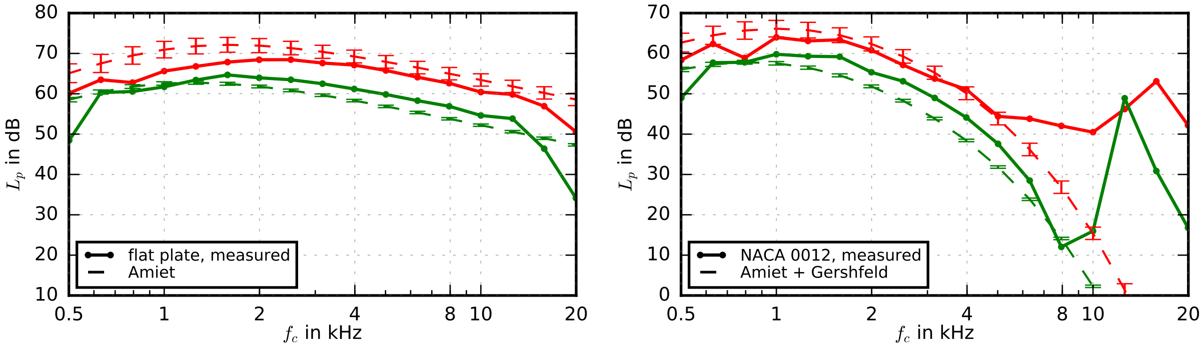

(a) Flat plate (b) NACA 0012 airfoil

Figure 7: Comparison of the acoustic results (solid lines) with the prediction using Amiet's model [1] and the correction from Gershfeld [4] (dashed lines), red: anisotropic, inhomogeneous turbulence, green: isotropic, homogeneous turbulence

example [21])[1].

2.4 Comparison of predicted noise spectra with measured spectra

The turbulence parameters measured at the two distances from the grid using the quad-sensor vorticity probe were used as an input to Amiet's flat plate model as given by Eq. (1) and the resulting sound pressure level spectra were compared to the results from the acoustic measurements on both the flat plate and the NACA 0012 airfoil. The comparison is shown in Fig. 7(a) for the flat plate and Fig. 7(b) for the airfoil[2]. In the latter case, the thickness correction proposed by Gershfeld [4] was additionally applied. Both figures contain the results from the measurements in isotropic, homogeneous turbulence (measured at a distance of 0.2 m from the grid) and those from measurements in quasi anisotropic, inhomogenous turbulence (at the shorter distance of 0.086 m from the grid). Additionally, the predictions contain an error bar indicating the resulting error when the standard deviations of the measured turbulence parameters U_x, Tu and Λ_x from their average values are assumed. Since the turbulence intensity and the mean flow speed are higher in close proximity to the grid than at the larger distance, the sound pressure levels (both measured and predicted) are also higher in the case of anisotropic, inhomogeneous turbulence.

For the flat plate (Fig. 7(a)), a sufficient agreement between the prediction and the measurements can be seen for both homogeneous, isotropic turbulence and inhomogeneous, anisotropic turbulence. In the first case, the flat-plate model underpredicts the noise by up to 3 dB for third octave band frequencies between 1.25 kHz and 12 kHz. In the latter case, the prediction exceeds the measured noise in the complete range of frequencies. For medium to high frequencies (2 kHz to 16 kHz) the difference in sound pressure level is again about 3 dB. The addition of the thickness correction method proposed by Gershfeld [4] to the noise prediction for the NACA 0012 airfoil (Fig. 7(b)) basically leads to the fact that the predicted spectra decrease sharply for frequencies approximately above 1.25 kHz. In the case of homogeneous and isotropic turbulence, the model yields sound pressure levels below the measured levels, with differences up to 6 dB for center frequencies from 800 Hz to 6.3 kHz. At higher frequencies, the measured spectra show a sharp peak, which is generated by the thin wire that holds the flat plate/airfoil. This is only visible in the results obtained for the airfoil, since for the flat plate case this noise contribution is masked by the considerably higher turbulence interaction noise levels. For the case of inhomogeneous and anisotropic turbulence, a sufficient agreement between prediction and measurement is only visibly for frequencies up to approximately 5 kHz. For higher frequencies up to 10 kHz, the predicted levels strongly decrease, while the measured levels decrease only slightly, leading to an increase of the difference between model and measurement. When examining the corresponding soundmaps (Fig. 6) it appears that the increase of the measured noise in inhomogeneous and anisotropic turbulence is a

[1]The tripping did have an influence when the noise generated at the trailing edge was examined.

[2]As a side note, the results of the flat-plate model based on input parameters obtained from the measurements with the single-wire probe were practically identical to those obtained with the quad-sensor vorticity probe in the present measurements.

residue of noise generated by the turbulence grid. With further increasing frequency, the spectra feature the noise peak generated by the thin wires.

Overall, the present comparison between predicted sound pressure levels and the results from the preliminary acoustic measurements can be summarized as follows:

1. Even at a distance of less than ten mesh widths downstream from the turbulence grid the anisotropy is weak.
2. The effects due to the inhomogeneity at this distance can be compensated for by performing several measurements in a plane normal to the flow. With the present setup, even a small number of about 15 measurements gives a consistent estimate of the turbulence parameters.
3. For the flat plate, Amiet's model as given by Eq. (1) gives sound pressure levels close to the measured values in a wide range of medium to high frequencies.
4. For the NACA 0012 airfoil, Amiet's model in combination with the thickness correction proposed by Gershfeld [4] leads to equally good estimates at medium frequencies. At high frequencies, noise generated by the turbulence grid as well as noise generated by the thin wires that hold the airfoil in the present experimental setup lead to larger deviations.

3. FINAL MEASUREMENTS

Based on the results from the preliminary measurements, a new set of measurements were performed on both the flat plate and the NACA 0012 airfoil at a larger number of flow speeds.

3.1 Parameters of inflow turbulence

Two different grids were used to generate the required inflow turbulence. The first grid, PPS 12/2, is the same square mesh grid that was used for the preliminary measurements. The second grid, called PPS 14/4, is also a perforated plate with square holes, but the mesh width is 14 mm and the bar width is 4 mm, with a resulting grid porosity of only 0.51. Details of both grids are given in Tab. 1.

In the new experiments, the parameters of the incident turbulence were determined at 30 measurement positions, randomly distributed in a plane normal to the flow with a size of 56 mm × 56 mm (corresponding to 4 mesh widths × 4 mesh widths of the second turbulence grid). The measurements were performed using a single-wire hot-wire probe with a sampling frequency of 25.6 kHz and a duration of 12 s. Apart from the probe, the same hardware was used for these measurements as for the preliminary measurements. Again, the first 2 s of the recorded data were omitted to avoid the possible influence of vibrations of the traverse system after each step.

From the remaining 10 s of data, the turbulence intensity Tu was again calculated according to Eq. (3) while the integral length scale was obtained by fitting the measured velocity spectra to the formulation for isotropic turbulence according to Eq. (7). The results are given in Fig. 8. It is visible that the turbulence intensity is higher closer to the grid (at a distance of 0.086 m) than further downstream (at a distance of 0.2 m), while the integral length scale is larger when further away from the grids.

3.2 Acoustic results

The flat plate used for the final measurements had the same thickness and span width as the one used for the preliminary measurements, but a shorter chord length of only 0.12 m. Thus, it had the same chord length as the NACA 0012 airfoil, which was the same as in the preliminary measurements. A thin strip of tripping tape was applied to both the flat plate and the airfoil. The rest of the setup and the data processing of the acoustic measurements was identical to that used for the preliminary measurements.

To account for the differences in the turbulent inflow conditions, the measured third-octave band sound pressure levels are scaled according to

$$L_{p,\mathrm{scaled}} = L_p - \left[10 \cdot \log_{10} Ma^5 + 10 \cdot \log_{10} Tu^2 + 10 \cdot \log_{10} \left(\frac{\Lambda_x}{c_l}\right)\right] \ \mathrm{dB}. \tag{11}$$

This scaling is based on the dependencies used in Amiet's high frequency solution as given in Eq. (1), although in the present case the integral length scale Λ_x was non-dimensionalized using the chord length c_l

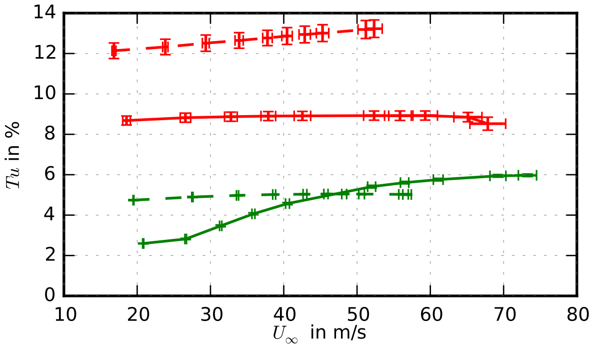

(a) Turbulence intensity

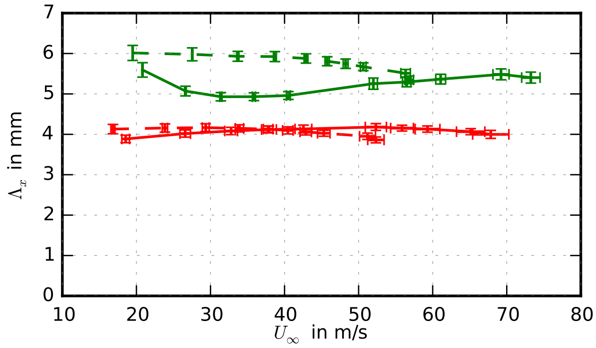

(b) Integral length scale

Figure 8: Properties of the turbulent inflow generated by the two perforated plates given in Tab.1, measured at 30 points in a plane normal to the flow (given is the mean value as well as the standard deviation), solid line: PPS 12/2, dashed line: PPS 14/4, red: anisotropic, inhomogeneous turbulence, green: isotropic, homogeneous turbulence

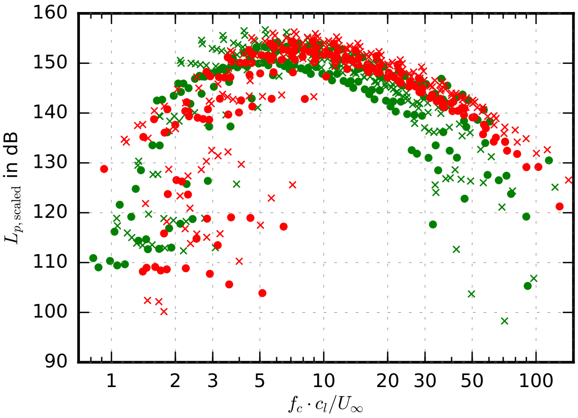

(a) Flat plate

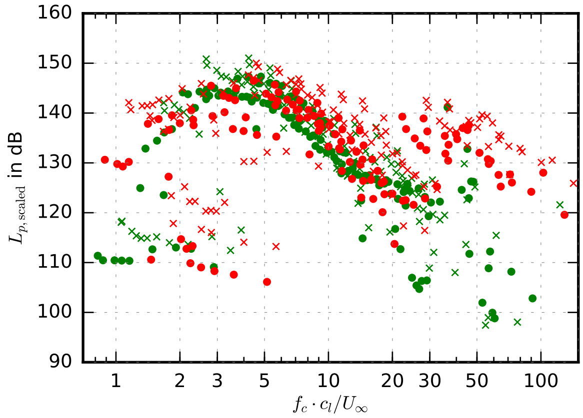

(b) NACA 0012 airfoil

Figure 9: Measured third-octave band sound pressure levels, scaled according to Eq. (11), as a function of the chord-based Strouhal number (red: anisotropic, inhomogeneous turbulence, green: isotropic, homogeneous turbulence, ● PPS 12/2, **x** PPS 14/4)

instead of the observer distance. The results are shown as a function of the chord-based Strouhal number $f_c \cdot c_l/U_\infty$ in Fig. 9(a) for the flat plate and in Fig. 9(b) for the NACA 0012 airfoil. Basically, a good collapse of the measured data is visible for the flat plate, especially at Strouhal numbers approximately above 5. In case of the NACA 0012 airfoil, the spectra scaled according to Eq. (11) still show considerable scatter. This is mainly true at high frequencies, and thus it may be caused by noise from the turbulence grid and the thin wires of the present experimental setup (as seen in Fig. 6 and, subsequently, Fig. 7(b)).

4. CONCLUSIONS

Using experimental data from measurements in a small anechoic wind tunnel, the present study describes methods to characterize the properties of both homogeneous, isotropic turbulence as well as inhomogeneous, anisotropic turbulence. In the present case, however, the anisotropy of the turbulence is weak even in a distance of considerably less than ten mesh widths downstream from the grid. The inhomogeneity can be taken into account by performing several measurements in a plane normal to the flow, although a good estimate can already be obtained with only about 15 measurements. A comparison of spectra predicted using a common flat-plate model for turbulence interaction noise with those obtained with microphone array measurements showed basically good agreement at medium and high frequencies. For the flat plate, the model overpredicts the noise by about 3 dB in the case of homogeneous, isotropic turbulence, while it underpredicts the noise by about the same amount in inhomogeneous, anisotropic turbulence. In case of the NACA 0012 airfoil, good agreement can be obtained only if a thickness correction is applied to the prediction.

After the description of the methodology and a basic validation using the preliminary measurements, a larger set of measurements was performed, again on a flat plate and a NACA 0012 airfoil in turbulent flows with different properties. The resulting sound pressure levels were scaled with the properties of the turbulent inflow. This was found to work well for the flat plate, while larger deviations were visible for the NACA 0012 data.

Acknowledgements

The authors thank Daniel Materne and Philipp Markus for their help with the measurements.

REFERENCES

[1] R. K. Amiet. Acoustic radiation from an airfoil in a turbulent stream. *J Sound Vib*, 41(4):407–420, 1975.

[2] M. R. Fink. Experimental evaluation of trailing edge and incidence fluctuation noise theories. In *Proceedings of the 13th AIAA Aerospace Sciences Meeting, AIAA paper 75-206*, 1975.

[3] J. O. Hinze. *Turbulence, Second Edition*. McGraw-Hill, New York, 1975.

[4] J. Gershfeld. Leading edge noise from thick foils in turbulent flows. *J Acoust Soc Am*, 116(3):1416–1426, 2004.

[5] R. W. Paterson and R. K. Amiet. Acoustic radiation and surface pressure characteristics of an airfoil due to incident turbulence. Technical report, NASA Contractor Report CR-2733, 1976.

[6] L. D. Santana, C. Schram, and W. Desmet. Low-frequency extension of Amiet's theory for compact airfoil noise predictions. *J Sound and Vib*, 372:342–356, 2016.

[7] K. Kucukcoskun, J. Christophe, C. Schram, J. Anthoine, and M. Tournour. An extension of Amiet's theory for spanwise-varying incident turbulence and broadband noise scattering using a boundary element method. In *Proceedings of the 16th AIAA/CEAS Aeroacoustics Conference, AIAA paper 2010-3987*, 2010.

[8] E. Sarradj, C. Fritzsche, T. F. Geyer, and J. Giesler. Acoustic and aerodynamic design and characterization of a small-scale aeroacoustic wind tunnel. *Appl Acoust*, 70:1073–1080, 2009.

[9] P. W. Roach. The generation of nearly isotropic turbulence by means of grids. *Int J Heat Fluid Flow*, 8(2):82–92, 1987.

[10] K. S. Wittmer, W. J. Devenport, and J. S. Zsoldos. A four-sensor hot-wire probe system for three-component velocity measurement. *Exp Fluids*, 24:416–423, 1998.

[11] T. F. Geyer, E. Sarradj, and J. Giesler. Application of a beamforming technique to the measurement of airfoil leading edge noise. *Adv Acoust Vib*, Vol. 2012, Article ID 905461, 2012.

[12] E. Sarradj and T. F. Geyer. Symbolic regression modeling of noise generation at porous airfoils. *J Sound Vib*, 333 (14):3189–3202, 2014.

[13] T. Kurian and J. H. M. Fransson. Grid-generated turbulence revisited. *Fluid dynamics research*, 41(2):021403, 2009.

[14] J. Jovanović. *The statistical dynamics of turbulence*. Springer, 2003.

[15] I. J. Sharland. Sources of noise in axial flow fans. *J Sound Vib*, 3:302–322, 1964.

[16] W. J. Devenport, J. K. Staubs, and S. A. L. Glegg. Sound radiation from real airfoils in turbulence. *J Sound Vib*, 329:3470–3483, 2010.

[17] P. Sijtsma. CLEAN based on spatial source coherence. *Int J Aeroacoustics*, 6(4):357–374, 2007.

[18] G. Herold and E. Sarradj. An approach to estimate the reliability of microphone array methods. In *Proceedings of the 21st AIAA/CEAS Aeroacoustics Conference, AIAA paper 2015-2977*, 2015.

[19] E. Sarradj. Three-dimensional acoustic source mapping with different beamforming steering vector formulations. *Adv Acoust Vib*, Vol. 2012, Article ID 292695, 2012.

[20] E. Sarradj. A fast ray casting method for sound refraction at shear layers. In *Proceedings of the 22nd AIAA/CEAS Aeroacoustics Conference, AIAA paper 2016-2762*, 2016.

[21] F. V. Hutcheson, T. F. Brooks, and D. J. Stead. Measurement of the noise resulting from the interaction of turbulence with a lifting surface. *Int J Aeroacoustics*, 11 (5,6):675 – 700, 2012.